

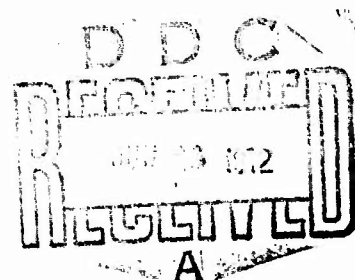
AD743738

# NAVAL POSTGRADUATE SCHOOL

## Monterey, California



# THESIS



The Effect of Ionospheric Tilt on  
Radio Direction Finding Position Estimates

by

Roger Kenneth Lunde

Thesis Advisor:

Robert R. Read

March 1972

Reproduced by  
NATIONAL TECHNICAL  
INFORMATION SERVICE  
Springfield, Va. 22151

Approved for public release; distribution unlimited.

59

## DOCUMENT CONTROL DATA - R &amp; D

(Security classification of title, body of abstract and indexing annotation must be entered when the overall report is classified)

1. ORIGINATING ACTIVITY (Corporate author) Naval Postgraduate School Monterey, California 93940		2a. REPORT SECURITY CLASSIFICATION Unclassified	
		2b. GROUP	
3. REPORT TITLE The Effect of Ionospheric Tilt on Radio Direction Finding Position Estimates			
4. DESCRIPTIVE NOTES (Type of report and, inclusive dates) Master's Thesis; March 1972			
5. AUTHOR(S) (First name, middle initial, last name) Roger Kenneth Lunde			
6. REPORT DATE March 1972		7a. TOTAL NO. OF PAGES 59	7b. NO. OF REFS 29
8a. CONTRACT OR GRANT NO.		9a. ORIGINATOR'S REPORT NUMBER(S)	
b. PROJECT NO.			
c.		9b. OTHER REPORT NO(S) (Any other numbers that may be assigned this report)	
d.			
10. DISTRIBUTION STATEMENT This document has been approved for public release and sale; its distribution is unlimited.			
11. SUPPLEMENTARY NOTES		12. SPONSORING MILITARY ACTIVITY Naval Postgraduate School Monterey, California 93940	
13. ABSTRACT It is generally accepted that the ionosphere tilts; that is to say, an isoionic layer is not at constant height above the surface of the earth. Ionospheric tilt has the effect of deflecting a radio ray out of its great-circle plane and returning it to earth at an angle not that of the true bearing from a receiver to a transmitter. The magnitude of error introduced by this effect on radio direction finding (RDF) position estimates was studied, in this paper. A model assigning a tilt bias of less than three degrees to each RDF station bearing was constructed. Analysis of a six-sta- tion RDF network revealed that this amount of tilt has neg- ligible effect on point estimates of location and their confidence regions.			

14.		KEY WORDS		LINK A		LINK B		LINK C	
				ROLE	WT	ROLE	WT	ROLE	WT
		Direction Finding							
		Position Finding							
		Ionospheric tilt							

The Effect of Ionospheric Tilt on  
Radio Direction Finding Position Estimates

by

Roger Kenneth Lunde  
Lieutenant Commander, United States Navy  
B.S., United States Naval Academy, 1964

Submitted in partial fulfillment of the  
requirements for the degree of

MASTER OF SCIENCE IN OPERATIONS RESEARCH

from the  
NAVAL POSTGRADUATE SCHOOL  
March 1972

Author

Roger K. Lunde

Approved by:

R R Read

Thesis Advisor

Jack P. Bortner

Chairman, Department of Operations Research  
and Administrative Sciences

Milton W. Chesser

Academic Dean

## ABSTRACT

It is generally accepted that the ionosphere tilts; that is to say, an isoionic layer is not at constant height above the surface of the earth. Ionospheric tilt has the effect of deflecting a radio ray out of its great-circle plane and returning it to earth at an angle not that of the true bearing from a receiver to a transmitter. The magnitude of error introduced by this effect on radio direction finding (RDF) position estimates was studied in this paper. A model assigning a tilt bias of less than three degrees to each RDF station bearing was constructed. Analysis of a six-station RDF network revealed that this amount of tilt has negligible effect on point estimates of location and their confidence regions.

## TABLE OF CONTENTS

I.	INTRODUCTION -----	6
II.	IONOSPHERIC PHENOMENA -----	8
	A. GENERAL DISCUSSION -----	8
	B. REMARKS ON PROPAGATION -----	8
	C. FIRST-ORDER SOLAR EFFECTS -----	11
	D. TRAVELING WAVE DISTURBANCES -----	14
	E. EXPERIMENTAL SUPPORT OF THE TILT CONCEPT -----	15
III.	THE MODEL -----	20
	A. QUALITATIVE FEATURES -----	20
	B. QUANTITATIVE FEATURES -----	23
IV.	COMPUTER SYNTHESIS -----	25
V.	SIMULATION -----	27
VI.	RESULTS AND ANALYSIS -----	28
VII.	CONCLUSIONS -----	30
VIII.	REMARKS -----	31
IX.	SUGGESTIONS FOR FURTHER STUDY -----	33
	APPENDIX A - TABLES -----	41
	LIST OF REFERENCES -----	54
	INITIAL DISTRIBUTION LIST -----	
	FORM DD 1473 -----	

## LIST OF FIGURES

1. RADIO RAY PROPAGATION MODES -----	10
2. THE EFFECT OF TILT ON REFLECTION OF A RAY FROM IONOSPHERE -----	12
3a. SIDE VIEW AT RECEIVER SHOWING ELEVATION ANGLE OF PROPAGATION MODES -----	13
3b. TOP VIEW AT RECEIVER SHOWING AZIMUTHS FOR DIFFERENT MODES -----	13
4. PLOT OF DATA COLLECTED BY SWEENEY (1970) -----	17
5. PLOT OF DATA COLLECTED BY SWEENEY (1970) -----	18
6. BASIC STEPS IN COMPUTER SIMULATION -----	26
7. PLOT OF 100 FIXES (ATLANTIC) -----	34
8. PLOT OF 100 FIXES (ATLANTIC) -----	35
9. PLOT OF 100 FIXES (OMAHA) -----	36
10. PLOT OF 100 FIXES (OMAHA) -----	37
11. PLOT OF 100 FIXES (GIMLI) -----	38
12. PLOT OF 100 FIXES (GIMLI) -----	39
13. DISPLACEMENT BY A 32 DEGREE ROTATION OF AXIS -----	40

## LIST OF TABLES

I.	COMPONENT OF BEARING ERROR DUE TO IONOSPHERIC TILT -----	41
II.	COMPOSITION OF RDF NETWORK FOR SIMULATION -----	42
III.	TARGETS USED IN SIMULATION -----	42
IV.	SAMPLE MEANS AND STANDARD DEVIATIONS (OMAHA) ----	43
V.	SAMPLE MEANS AND STANDARD DEVIATIONS (OMAHA) ----	44
VI.	SAMPLE MEANS AND STANDARD DEVIATIONS(ATLANTIC) --	45
VII.	SAMPLE MEANS AND STANDARD DEVIATIONS(ATLANTIC) --	46
VIII.	SAMPLE MEANS AND STANDARD DEVIATIONS (PACIFIC) --	47
IX.	SAMPLE MEANS AND STANDARD DEVIATIONS (PACIFIC) --	48
X.	SAMPLE MEANS AND STANDARD DEVIATIONS (GIMLI) ----	49
XI.	SAMPLE MEANS AND STANDARD DEVIATIONS (GIMLI) ----	50
XII.	SAMPLE MEANS AND STANDARD DEVIATIONS(VERACRUZ) --	51
XIII.	SAMPLE MEANS AND STANDARD DEVIATIONS(VERACRUZ) --	52
XIV.	REDUCED LOCATION DATA FOR THE OMAHA SAMPLES -----	53

## I. INTRODUCTION

Long range radio direction finding (RDF) is the art of determining the geographical position of a transmitter of unknown location by measuring the azimuthal angle of arrival (bearing) of a radio ray at several receiver sites and estimating the location of the transmitter by a form of triangulation. RDF techniques typically are based on the following two assumptions: 1) The earth is modeled sufficiently well by a true sphere, and 2) An observed bearing varies from true bearing by random error which is distributed normally (gaussian) with mean zero. The model is  $O = T + e$ , where  $O$  = observed bearing,  $T$  = true bearing and  $e$  = normal error associated with the receiver.

This investigation was concerned with the possibility of the existence of a non-trivial error due to ionospheric reflection superimposed on true bearing. The model hypothesized was  $O = T + B + e$ , where  $B$  is a random variable which is normally distributed about a non-zero mean. This component changes the mean of the distribution of the observed bearings from  $T$  to  $T + b$ , where  $b$  is the mean of  $B$ .

It is well known that reflecting layers in the ionosphere are not of equal height above the surface of the earth. This produces an ionospheric tilt which can provide

the component B. There are at least two major obstacles to modeling this effect:

- 1) Non-predictable traveling wave disturbances and the random phenomena which produce them keep the ionosphere in a constant state of flux, and

- 2) There does not exist a sufficiently extensive monitoring network to completely map electron densities in the ionosphere. These obstacles are discussed in the sequel together with general discussion on the effects of ionospheric tilt on RDF bearings and the estimated positions derived from those bearings. A model is presented and computer simulation is used to demonstrate the tilt effect on estimated location and confidence regions.

## II. IONOSPHERIC PHENOMENA

### A. GENERAL DISCUSSION

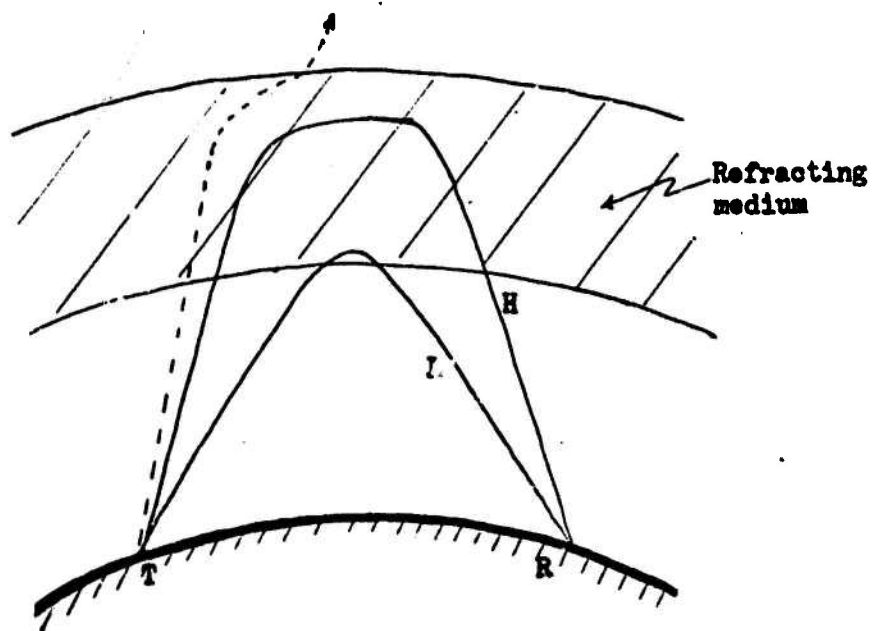
The ionosphere is a region of electrically charged (ionized) air beginning about 25 miles above the surface of the earth. Radio waves can travel long distances by being refracted in the ionosphere and returned to earth. It is the refracted ray that is received at the RDF site. The degree of ionization and the distribution of the charged particles is not constant with respect either to time or geographical location. This inconsistency results in refraction of a ray in a different manner from one instant of time to another for a given signal over a given path.

Very grossly the ionosphere may be thought of as a sea; that is, layers are not completely flat but contain ripples like waves on an ocean. In addition to the small-scale phenomena that compound inconsistent refraction: 1) First-order solar effects and 2) Traveling wave disturbances. The nature and effect of these concepts are discussed first followed by citation of some experimental support.

### B. REMARKS ON PROPAGATION

Although it is convenient to think of the ionosphere as a mirror-like reflecting surface, and such an interpretation is sufficient for some purposes, in actuality rays are bent or refracted in the ionosphere before being returned to earth. The amount of bending or the time a ray spends

in the ionosphere before being returned to earth depends in a complicated way on wave frequency, magnetic field and depth of penetration. In Figure 1, L represents "low-angle" refraction and H "high-angle". It is seen that rays arrive at the receiver, R, at correspondingly different elevation (vertical angle). It is also intuitive that the high-angle ray spends more time in the ionosphere since it penetrates deeper. In the sequel, reference will be made to three layers, E, F1 and F2. In a smooth undisturbed ionosphere, the F layers typically reflect both a high and a low ray as in Figure 1 whereas the E layer typically reflects only one ray. Figure 1 illustrates "one-hop" transmission. Two-hop rays (and higher degree hops) result from reflection at the surface of the earth back into the ionosphere which again returns the ray to earth at a different geographical location. Terminologically, a one-hop low-angle ray reflected at the F1 region will be designated 1F1L. A two-hop F2 high-angle ray will be 2F2H. Similarly, 2E will refer a two-hop ray reflected at the E layer. For further treatment of propagation phenomena the reader is referred to any of the number of textbooks on the subject. Two texts recommended are Kelso (1964) and Davies (1965). Also Ames (1964) contains an excellent brief discussion of propagation relating to the effect of tilt on bearing angle.



Radio ray propagation modes

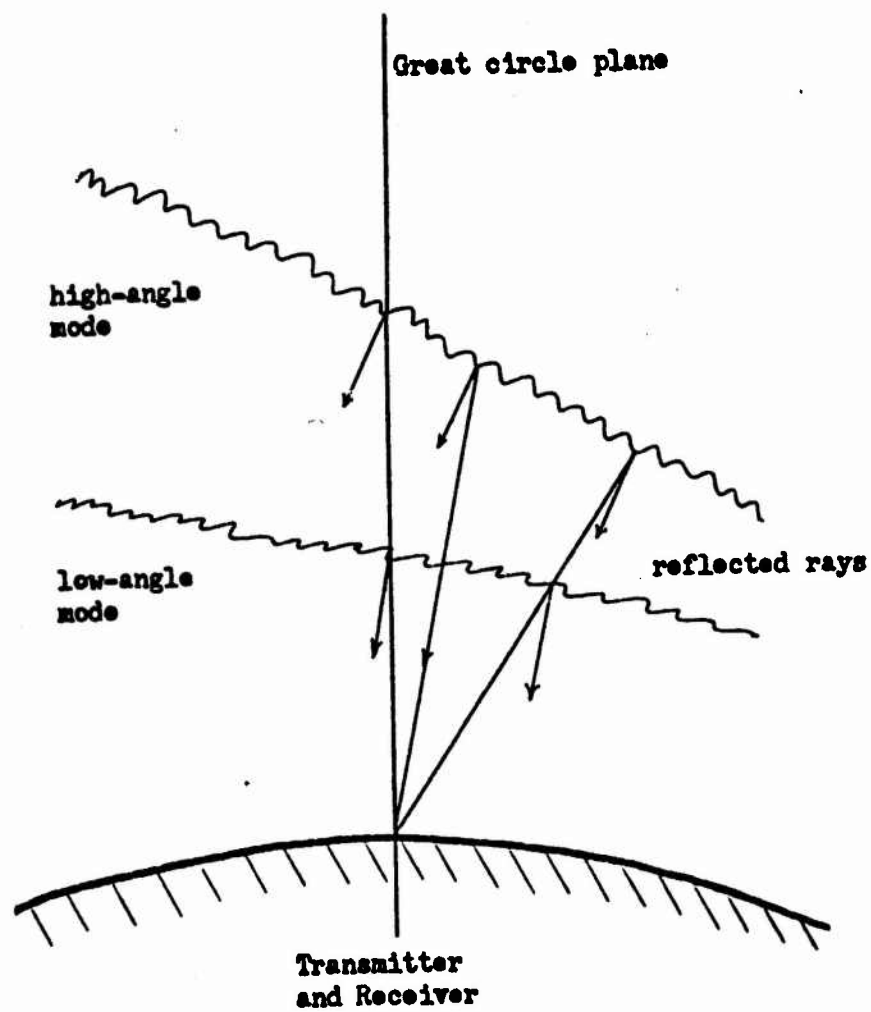
FIGURE 1

### C. FIRST ORDER SOLAR EFFECTS

Air particles in the ionosphere are ionized by ultraviolet rays from the sun and to a less extent by charged particles from the sun. Therefore the angle at which the sun's rays pass through the ionosphere determines the degree of ionization.

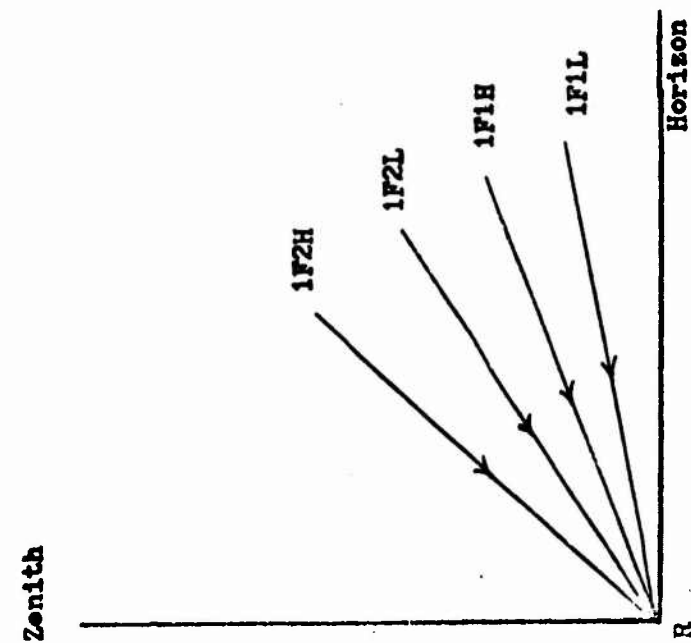
If allowed to ignore the effects of traveling disturbances, magnetism, earth surface and wind conditions one could say that an isoionic layer of the ionosphere is highest above the surface of the earth at the equator and decreases in altitude with increasing latitude because the angle between the sun's rays and local zenith increases as latitude increases. The result is a north-south tilt. Furthermore, ionization increases with increasing height and higher layers tilt more than lower layers. Figure 2 exaggerates the point. If the four possible rays reflected from the F layers are simultaneously received at one point one would expect each to arrive on a slightly different bearing. Figure 3a illustrates the difference in elevation angles and Figure 3b shows difference in azimuthal angles of arrival for the four rays.

In addition to this latitudinal effect there exists an east-west tilt. Electron density is highest at local noon and lowest at local midnight. There is constant change throughout the day and changes are very pronounced at ionospheric sunrise and sunset. Bramley (1956) estimated the east-west diurnal tilt change rate to be on the order



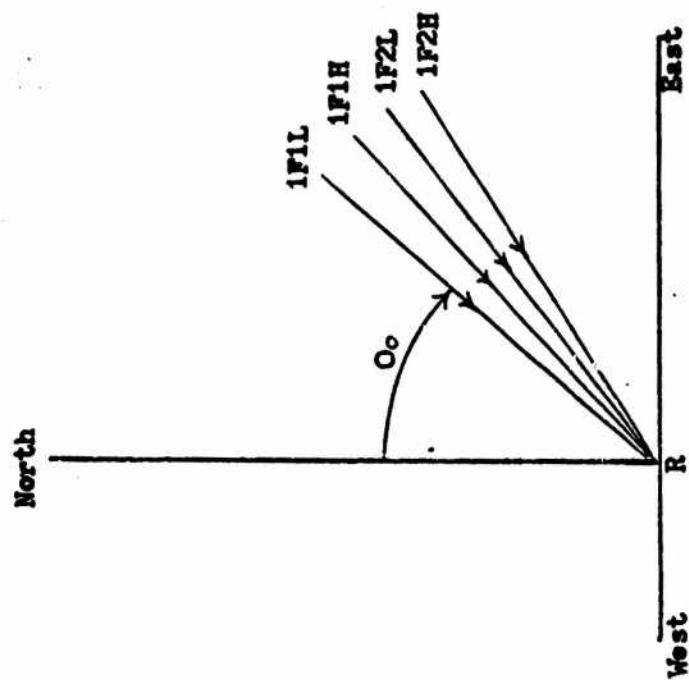
The effect of tilt on reflection  
of a ray from ionosphere

FIGURE 2



Side view at receiver showing  
elevation angle of propagation modes

a.



Top view at receiver showing  
azimuths for different modes

b.

FIGURE 3

of 0.2 degrees per hour. He does not distinguish between sunrise and sunset hours and periods of less change.

Similar to the diurnal tilt there exists a seasonal variation as the earth rotates around the sun and the sun's direct rays vary between the Tropic of Cancer and the Tropic of Capricorn. This effect is considered by most experimentors to be quite minor and slow to change compared to diurnal effects. Munro and Heisler (1963) summarize existing thought on the magnitude and directionality of both diurnal and seasonal effects.

#### D. TRAVELING WAVE DISTURBANCES

There are a number of other factors directly influencing the shape of an isoionic layer. The ionosphere over land is considerably different than it is over sea. The earth's magnetic field causes drag in the F-layer plasma and it varies highly. There are winds, thermal, and coriolis effects. One more phenomenon, traveling disturbances, will be discussed briefly.

Much literature exists on the subject of traveling wave disturbances. Several articles contain composite reviews of existing thought and past experiments and conclusions. One of the best of these is Detert (1965). (See also Munro and Heisler (1963) and Heisler (1965)).

A disturbance is characterized by an increase or decrease in electron density over background profiles. In early experiments traveling disturbances were included in a broad category called ionospheric storms. As more

sophisticated measuring equipment became available they became known as traveling wave disturbances and attempts were made to measure their size and velocities, and to predict them. A wide range of sizes and velocities have been reported. Hewish (1951, 1952) reports observing lengths (longitudinal extents) from 2-10 kilometers. Bramley (1953, 1955, 1956) observed velocities from 90 to 1300 km./hr. Chan and Villard (1962) reported disturbances from 1300 km. to over 2000 km. in length and velocities from 1450 to 2750 km./hr. Heisler (1963) shrewdly points out that size and velocity observations depend heavily on the method of measurement.

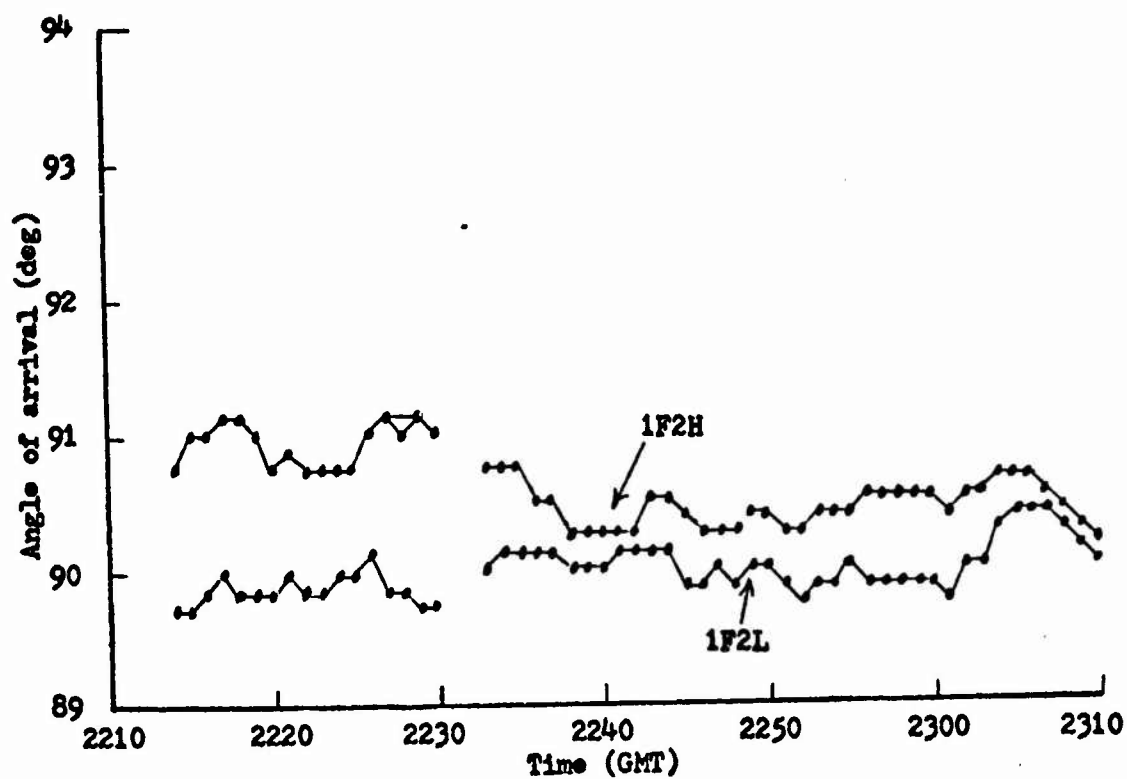
Causes of disturbances can be known (e.g., observable sun storms) or unknown. Chan and Villard believed the large disturbances they observed to have resulted from the same event that caused a coincidental change in the earth's magnetic field.

#### E. EXPERIMENTAL SUPPORT OF THE TILT CONCEPT

The results of three experiments will be presented in support of the existence of a non-zero mean bearing error. Sweeney (1970) measured the azimuthal pattern realized by a 256-element 2.5 km. broadside array receiving HF signals propagated over a 2600 km. east-west path. It was found that high rays tend to arrive south of low rays. Sweeney hypothesized that this tendency is a consequence of ionospheric tilts having north-south slopes which increase with altitude. This hypothesis was confirmed by

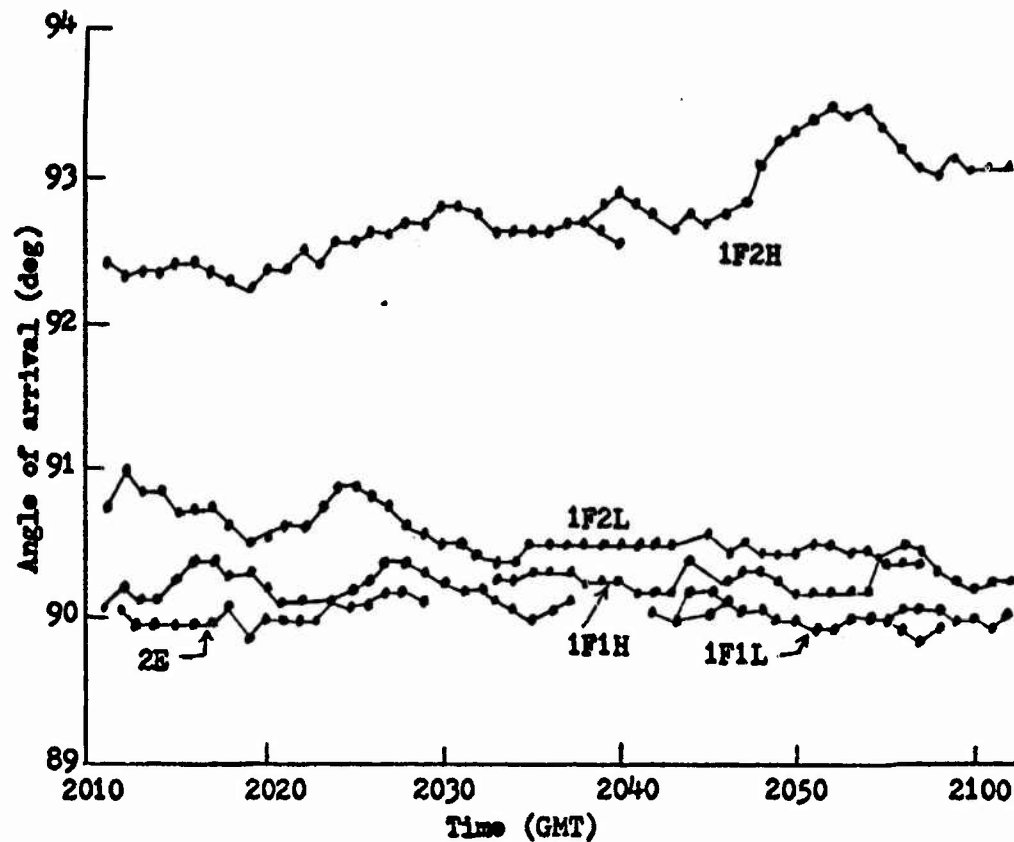
modeling the ionosphere in a computer ray-tracing program. Figure 4 and Figure 5 are reproduced from Sweeney's report. The true transmitter bearing was 90 degrees. In Figure 4 it can be seen that the 1F2L ray oscillates about the true bearing during undisturbed conditions. Sweeney summarizes that low-angle rays are accurate to the resolution of his antenna system; that is, one cannot discern a non-zero mean component of error in the low-angle rays. Sweeney also concludes that deviations occur mainly in reflection from the earth. If this is in fact the case one can draw the following conclusions: 1) deflection out of a great circle plane will not be measurable in a one-hop low-angle ray, 2) a high-angle ray will be observed noticeably south of the low-angle ray, and 3) multiple-hop rays will have more error due to reflections from the earth's surface. It must be kept in mind that Sweeney's two-hop rays were being reflected by the Rocky Mountains, an unusually rough reflecting surface.

Bredex (1963) was concerned with round-the-world (RTW) propagation. But his comments on the direct ray (Stanford, California to Champaign, Illinois) are of interest. The direct ray is defined to be the signal received via the shorter of the two great circle paths. Bredex observed that bearings fluctuated about a daily mean. The winter means were north of true bearing and displayed a southerly trend until they swung south of true bearing in March. With ten data points Bredex was able to fit a curve



Plot of data collected by Sweeney (1970) showing high-angle ray arriving south of low-angle ray. The data were taken at 23 MHz on 25 August 1969. True bearing was 90 degrees.

FIGURE 4



Plot of data collected by Sweeney (1970) illustrating the difference in azimuth of different propagation modes. The data were taken at 14.5 MHz on 30 September 1969. True bearing was 90 degrees.

FIGURE 5

which crossed true bearing on 21 March, the vernal equinox. The conclusion is obvious even if somewhat speculative. Mildly stated, bearing means are sensitive to seasonal change. One other Bredek observation is worth noting here. Variation in RTW bearings was centered "a few degrees" south of the direct bearings. This is consistent with Sweeney's conclusion. Since the RTW ray has traveled much farther than the direct ray and is definitely multi-hop one expects to observe more variation in it. And with Sweeney's hypothesis one expects it to arrive south of the direct ray.

An unpublished experiment conducted at Naval Security Group Activity, Skaggs Island, California, showed the existence of an east-west diurnal tilt. Bearings were taken at two minute intervals on a signal transmitted from Hawaii during ionospheric sunrise and sunset. The data were analyzed by an autocorrelation function. Over a period of two hours the bearings failed to become statistically independent; that is to say, the bearings showed a definite trend to slide in one direction and not fluctuate about a cumulative mean. Similar experiments were conducted during undisturbed day and night conditions. The results were similar to Bramley and Ross (1951). Bramley (1953, 1955) and Bain (1955). Bearings showed a slow (up to 20 minutes) quasi-cyclic fluctuation about a mean in addition to rapid second-to-second fluctuation.

### III. THE MODEL

There does exist a deterministic element of bearing error. At least it can be said that there exists a component of error that has a determinable non-zero mean. The goal of this thesis is to determine the effect of this non-zero mean component B on RDF "fixes" (estimated transmitter location) and probability statements about these fixes.

According to Dr. Villard<sup>1</sup> (private communication 30 November 1971) the present state of technology is such that the non-zero mean component can be measured to almost any accuracy desired. What is lacking is the total commitment of effort and equipment to measure such a bias. In the absence of this commitment one may account for the error by modeling and statistical methods.

#### A. QUALITATIVE FEATURES

The most severe effect of ionospheric tilt is from east-west tilt at ionospheric sunrise and sunset. At other times of the day east-west tilt is very gradual. No attempt is made to account for sunrise and sunset tilt in this model. It is suggested, however, that this tilt should be

---

<sup>1</sup>Dr. O. G. Villard, Jr., of Stanford University, is Chairman of the Special Committee on Electronics, a panel of the Naval Research Advisory Committee.

modeled by an error with positive mean for bearings in the third and fourth quadrants and a negative mean for bearings in the first and second quadrants at sunrise and oppositely at sunset. Between sunrise and sunset (and sunset and sunrise) east-west tilt is modeled sufficiently well with mean tilt equal to zero.

The degree of north-south tilt is more consistent than the diurnally periodic east-west tilt. The ionosphere tilts west to east in the morning and east to west in the afternoon whereas a north to south tilt exists throughout the day. In the sequel error due to tilt,  $B$ , is that produced by north-south tilt.

The model is restricted to rays reflected by an ionosphere between sunrise and sunset and to RDF stations and targets located in the northern hemisphere. It was constructed to represent conditions at mid-latitudes and it is assumed to be sufficiently accurate for all latitudes for which it is used in collection of data for this thesis.

The model contains two components of error. One is the usual random error and the other is due to tilt,  $B$ . The tilt component can be reduced to an unbiased random component by inserting a zero mean.

The model assigns a positive mean to error in bearings from zero to 180 degrees and a negative mean to bearings from 180 to 360 degrees. The error is assumed normal. Absolute value of the mean decreases with increasing distance due to the following two assumptions. It was assumed

that the receiver could not distinguish high-angle rays from low-angle rays. As a result the bearing measured is due to some unknown combination of high and low-angle rays. It was further assumed that the low-angle ray varies about the true bearing and the high-angle ray is the sole contributor to error due to tilt. High-angle rays are attenuated more rapidly than are low-angle rays. It follows that the greater the distance the less effect on bearing will there be due to the high-angle ray and the less the deviation due to tilt.

A systematic standard deviation is assigned to each RDF station. It is the basis of the dispersion of both random error,  $e$ , and tilt error,  $B$ . For use as a parameter in determining  $e$ , it increases with increasing distance (see Pope (1970)). For use as a parameter of  $B$  it decreases with increasing distance. Intuitively, the longer a ray is exposed to error-producing elements the more dispersion one expects in its distribution. This explains the increase of the parameter, call it  $s$ , with distance for  $e$ . A different argument applies to  $B$ . It is claimed that the dispersion of  $B$  is directly proportional to  $b$ , the mean of  $B$ . The quantity  $b$  is in some sense a measure of the strength of the effects that produce error due to tilt. The higher the value taken on by  $b$  the more influence on bearing has the high-angle ray. Using the same argument as for  $s$  (i.e., more exposure means higher variability) one concludes that the higher the  $b$  the greater the variance of

B. The parameter supplied in the model multiplies  $s$  by  $b$  to serve as the standard deviation of  $B$ . When  $b$  is zero due to great distance (complete attenuation of the high-angle ray)  $s$  is used as the standard deviation of  $B$ .

A final qualitative feature of the model recognizes the facts that mean error due to tilt is not the same for different bearings taken simultaneously from one site and tilt is not sloped exactly north-south. Predictions of actual slope at a given point in the ionosphere are extremely gross and quite inappropriate for a given instant of time. Also the high-angle ray is mixed with the low-angle ray in some unknown proportion. All of these effects are accounted for in the model by introducing a maximum value parameter  $b'$  (see Table 1) and multiplying it by a uniform random variable to produce  $b$ .

#### B. QUANTITATIVE FEATURES

The maximum  $b'$  was assigned values as a function of distance according to Table 1. The values were assigned with some uneasiness but an attempt to justify them follows.

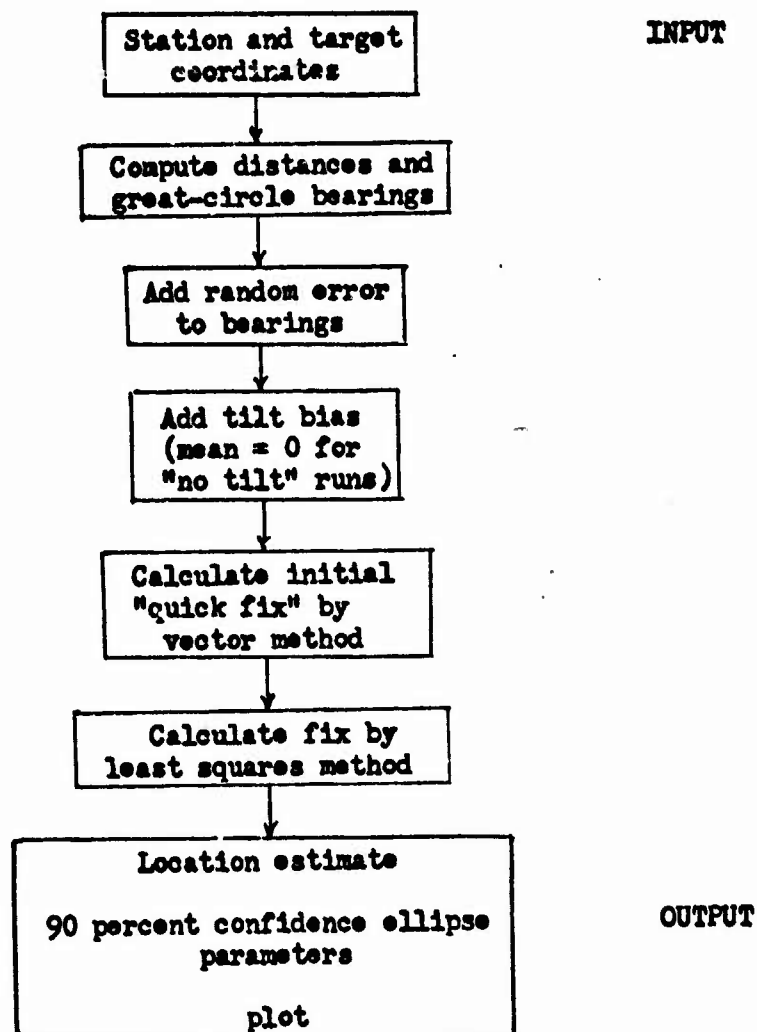
For distances less than 50 miles it was assumed that a ground wave is predominant and there is no effect from ionospheric tilt. At distances greater than 3600 miles the high-angle ray was assumed completely dissipated so that once again there is no deflection due to tilt.

Sweeney (1970) observed high-angle rays that arrived approximately three degrees south of low-angle rays along an east-west propagation path (see Figure 4 and Figure 5).

He modeled this phenomenon with an alpha-Chapman layer in the Jones (1966) three-dimensional ray-tracing computer program using average density data during undisturbed conditions. The results supported the hypothesis that the high-angle ray arrives approximately three degrees south of the low-angle ray for that particular 90 degree - 270 degree path. It is acknowledged that the maxima assigned to the distance categories between 900 miles and 3600 miles are artificial as are the categories themselves. But the assignments are sufficient to illustrate the effect of a component of error due to tilt and they are consistent with the qualitative discussion above.

#### IV. COMPUTER SYNTHESIS

The model was programmed in the Fortran IV language and computer simulation was employed to evaluate the effect of the non-zero component of error on the location of a fix point and the size and shape of the confidence regions generated by a standard RDF fix technique. Inputs to the program were station and target coordinates and a station systematic standard deviation. True bearings were computed and random and tilt error was superimposed on them. Fix points were computed by a vector method (Pope 1971) and the least squares method (Daniels, 1951 and Kukes and Starik, 1964). Two methods of obtaining confidence regions were available, chi-square regions and bivariate normal regions. Only the latter was used. Two random number generators were used to determine bearing error. One selected uniform random variates in the interval (0,1) while the other selected normal random variates for a given mean and standard deviation. Both generators are those recommended by Naylor, Balintfy, Burdick and Chu (1966). The basic steps in the simulation are shown in Figure 6.



Basic steps in computer simulation

FIGURE 6

## V. SIMULATION

A network of six RDF stations (Table II) took bearings on five targets (Table III). One hundred fixes were computed for each of the targets assigning only random error to the bearings. An additional 100 fixes were computed for each target with the model assigning to each bearing a component of error due to ionospheric tilt. For each set of 100 fixes, means and standard deviations were computed for latitude and longitude of the fix point and the major semiaxis and minor semiaxis and axis of rotation of the 90 percent confidence ellipse. Additionally, the fix points were plotted on a graph with rectangular coordinates. This procedure was repeated 25 times for each target.

## VI. RESULTS AND ANALYSIS

The sample means and standard deviations for each simulation run were tabulated in Tables IV to XIII. Figures 7 through 12 are selected samples of plots of fix locations. Meaningful statistical inferences and the validity of the model require that the samples collected be random. But the sample mean latitudes for Omaha, Gimli and Veracruz follow a definite trend and overwhelmingly fail the run test for randomness. It is interesting to note that the mean latitudes for these three targets are the only sets of values that fail the test for randomness (with the exception of the very stable minor semiaxis values). Even for these targets the mean longitudes show no trend whatever. In order to more clearly determine the randomness of the samples of positions, it was observed that the data are matched pairs of latitude and longitude. The data were reduced to single observations  $D(1) = \text{longitude}(1) - \text{latitude}(1)$ . The  $D(1)$  for the Omaha samples are tabulated in Table XIV. At significance level .05 the hypothesis that the  $D(1)$  constitute a random sample is accepted.

The objective of this thesis has been met without further statistical examination. Differences between extreme mean locations measure in the low tenths of degrees, just several miles. The systematic effect of tilt is insignificant from a practical point of view.

One important observation is that the standard deviations of the Omaha axes of rotation are quite large. Although in the Omaha example major and minor semiaxes are quite similar in magnitude, a variation from one extreme rotation angle to the other involves a displacement of approximately 25 percent of the area of the confidence region (crossed area in Figure 13).

## VII. CONCLUSIONS

Fix points and confidence regions were calculated from sets of bearings containing only random error and compared to the points and regions calculated from sets of bearings to which a component of error due to ionospheric tilt had been added. This component was considered a normal random variable.

The effect of superimposing a tilt error on bearings on the least squares method of computing estimated location and confidence regions from a six-station RDF network is negligible for a mean error due to tilt of less than or equal to three degrees with standard deviation less than three degrees.

The most intriguing development was that only in the case where the target was completely surrounded by stations did the angular orientation of the confidence region vary appreciably. Tilt played no role in this variability.

### VIII. REMARKS

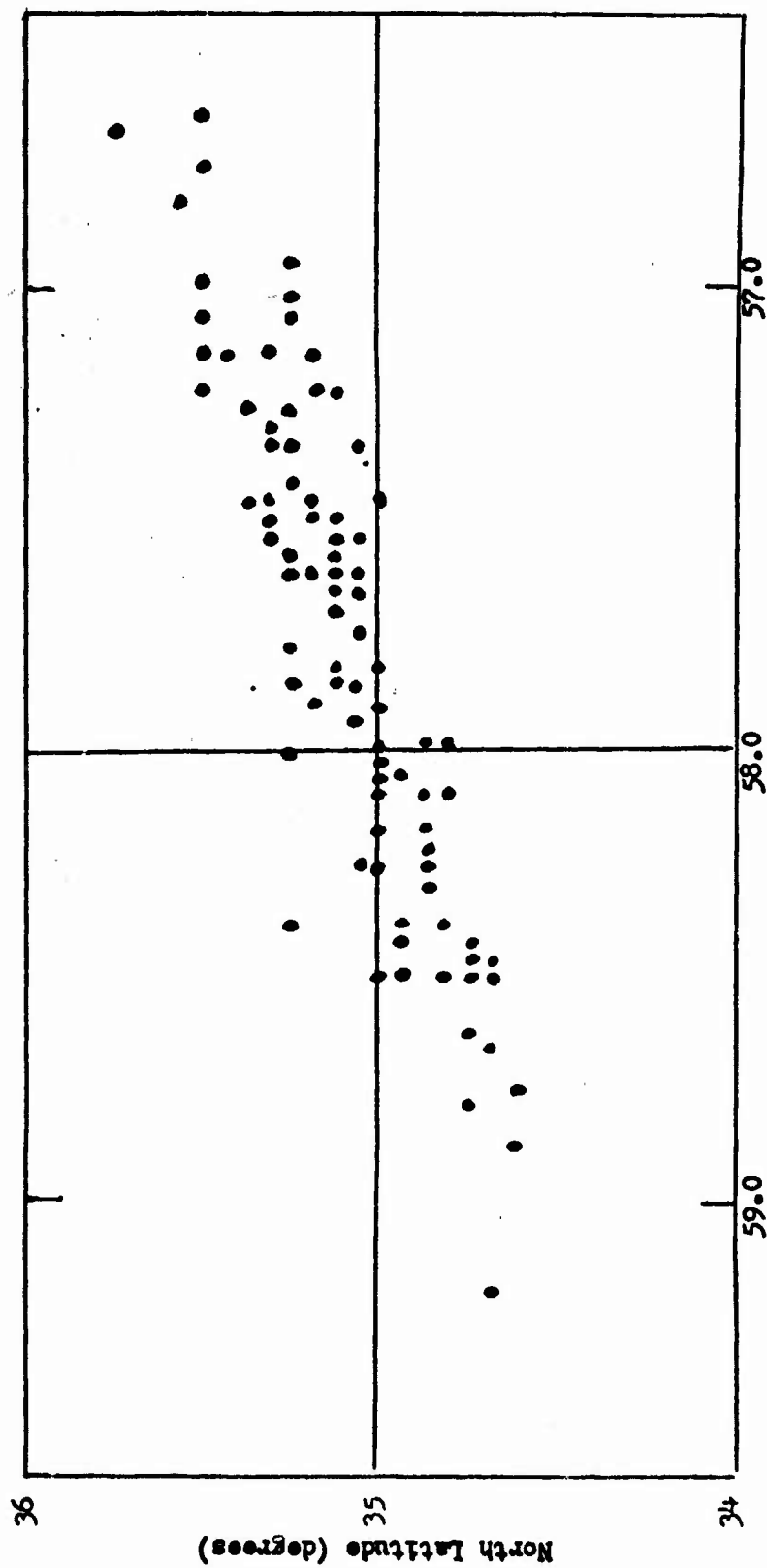
The model presented was only a gross approximation to the effect of tilt. There are ways available to more accurately model the ionosphere. Predictions of ionospheric characteristics exist in several forms. Ionospheric Predictions, published by the Institute for Telecommunications Sciences and Aeronomy (ITSA), is a monthly periodical which contains numerical maps of maximum usable frequency at zero range (MUF(ze-ro)) and MUF(4000km.) for the F2 layer. In conjunction with other publications (e.g., National Bureau of Standards (NBS) Circular 462) it is possible to approximate virtual height of the F2 layer with respect to geographical location and time of day. The NBS Technical Note 40 series is published quarterly and contains predictions of ionospheric electron density. These can be used to construct a model based on the Chapman layer. (See Barnum (1968) p. 75 and Haydon and Lucas (1968)) With these aids the ionosphere can be modeled more accurately but in view of the results of this thesis it is suggested that an attempt to do so for RDF objectives would prove unprofitable.

The mathematical treatment of the RDF problem is by no means new. The theory was well presented by Stansfield (1947) and Daniels (1951). Kukes and Starik (1964) present a more lengthy and detailed discussion of the same basic theory. Burt, Kaplan, Keenly, Reeves, and Shaffer

(1966) further defined terms and presented techniques for handling the general position finding problem. Existing techniques assume the earth to be a true sphere and employ spherical trigonometry. In fact, the earth is slightly oblate so that over long distances a correction to the spherical treatment is necessary for accurate location. In RDF the problem becomes the difference in bearing between a spherical great circle and a spheroidal geodesic. Using parameters for the Clark Spheroid of 1866 the difference at mid latitude was found to be as great as 0.5 degrees. An additional characteristic is that the geodesic may start north of the great circle then cross to south as distance increases. In practice the detrimental effect of the spherical assumption is considered negligible. Thomas (1970) discussed spheroids and presented solutions to a geodesic which are adaptable to both manual and computer calculation.

## IX. SUGGESTIONS FOR FURTHER STUDY

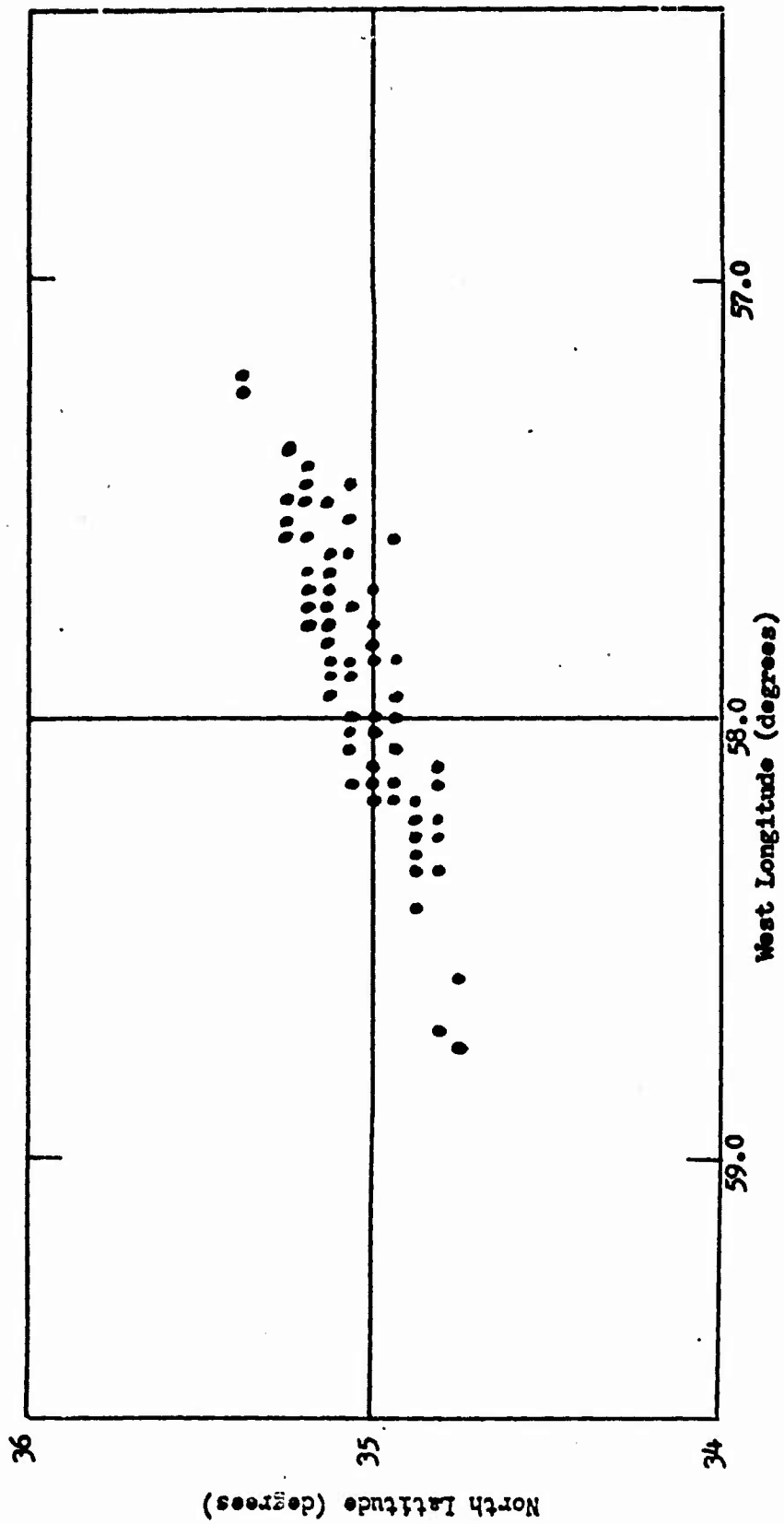
Although the cases simulated in this report were chosen to demonstrate the effect of tilt on RDF fix points, one interesting side-effect provided an outfall. The orientation of a confidence ellipse can change considerably the geographical area covered by that region. Furthermore, it appears that the variability of orientation depends on the location of the target relative to the RDF network. The variability of orientation of confidence regions can have tremendous impact on the validity of probability statements based on RDF techniques. A study of the effect on confidence regions of target location and network configuration is suggested. The orientation of a confidence region depends on the magnitude of variance of each bearing used to calculate the fix point. A study to determine the sensitivity of this orientation as a function of variance in individual bearings may prove valuable.



Plot of 100 fixes

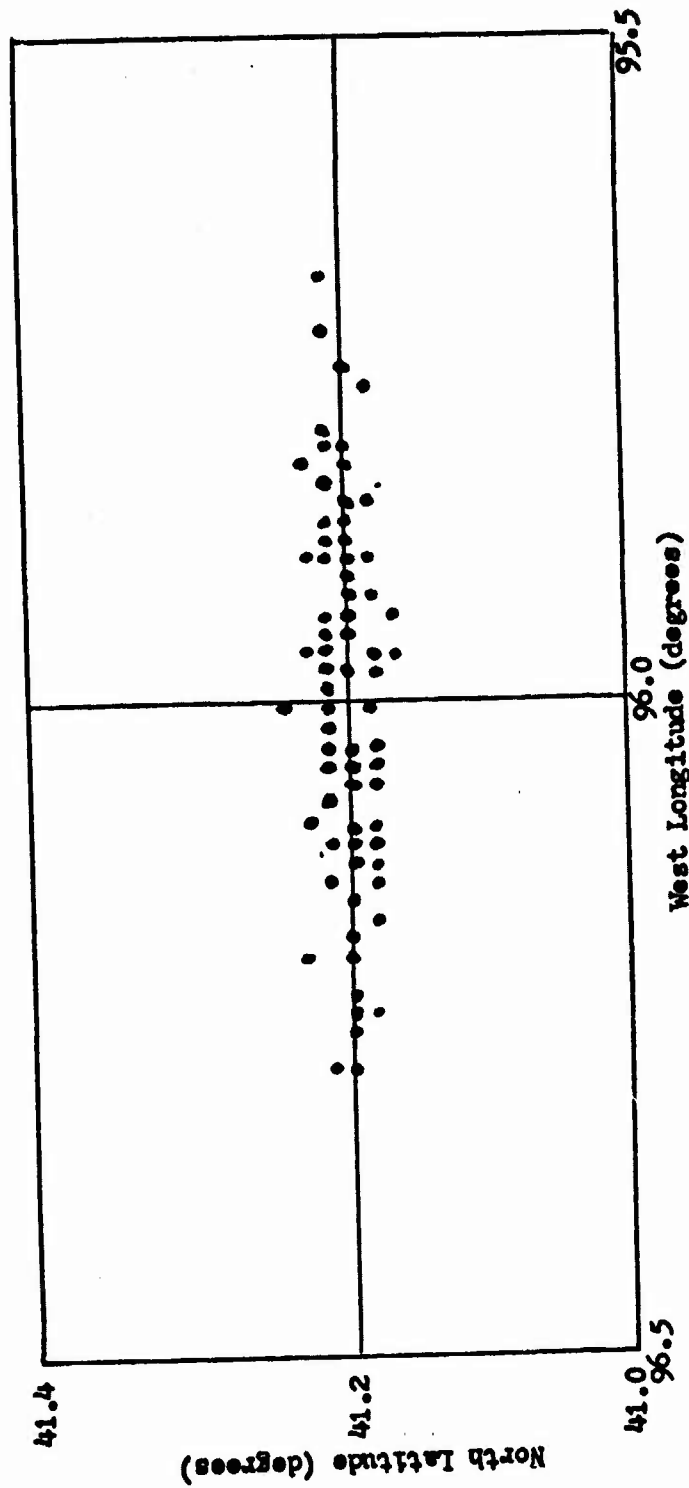
Target: Atlantic  
Mode: Tilt  
True position: 58.0W 35.0N

FIGURE 7



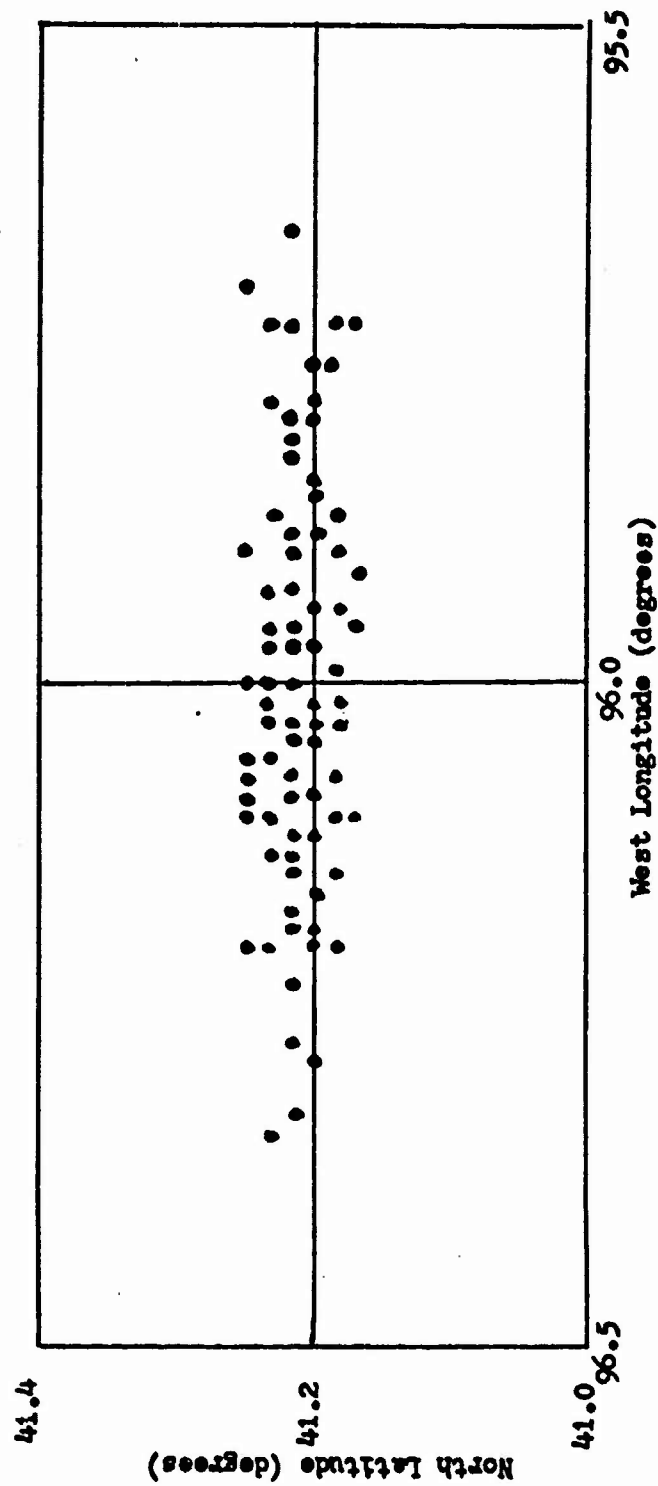
Plot of 100 fixes  
 Target: Atlantic  
 Mode: Tilt  
 True position: 58.0W 35.0N

FIGURE 8



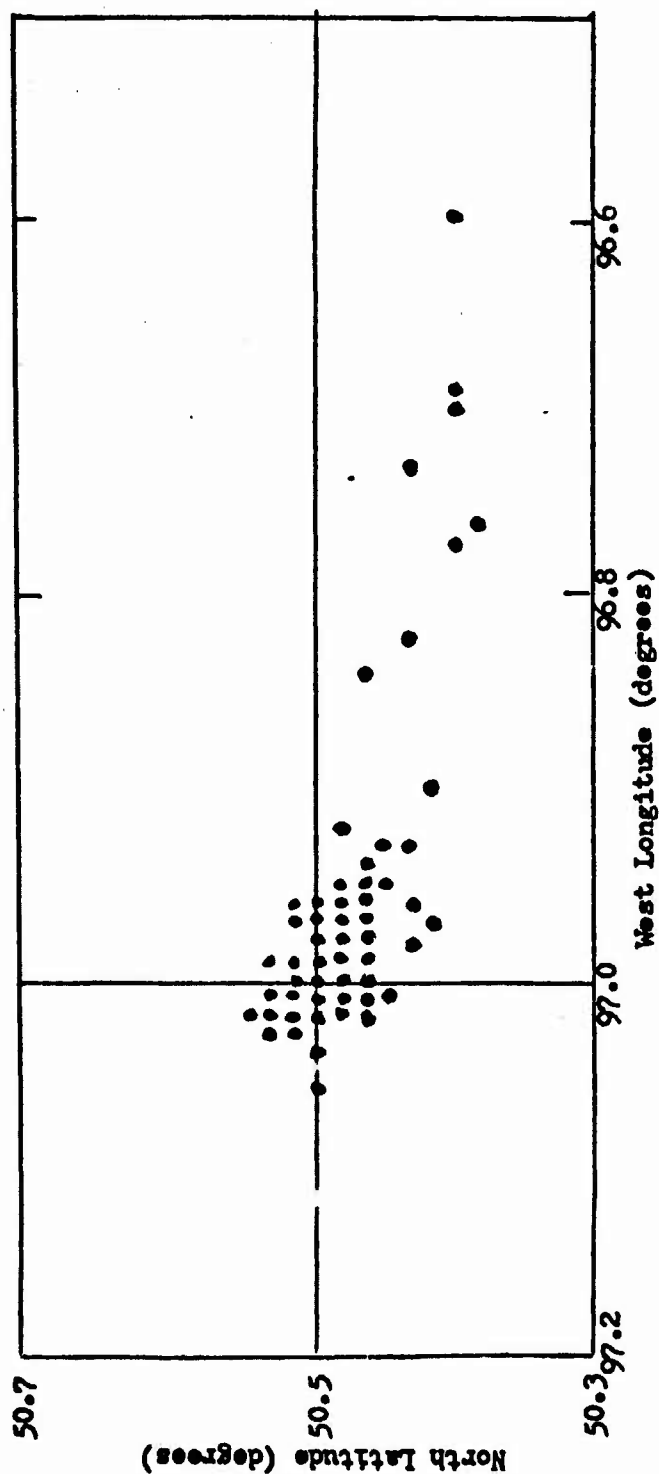
Plot of 100 fixes  
 Target: Omaha  
 Mode: Tilt  
 True position: 96.0W 41.2N

FIGURE 9



Plot of 100 fixes  
 Target: Omaha  
 Mode: No tilt  
 True position: 96.0W 41.2N

FIGURE 10



Plot of 100 fixes  
 Target: Gimli  
 Mode: No tilt  
 True position: 97.0W 50.5N

FIGURE 11

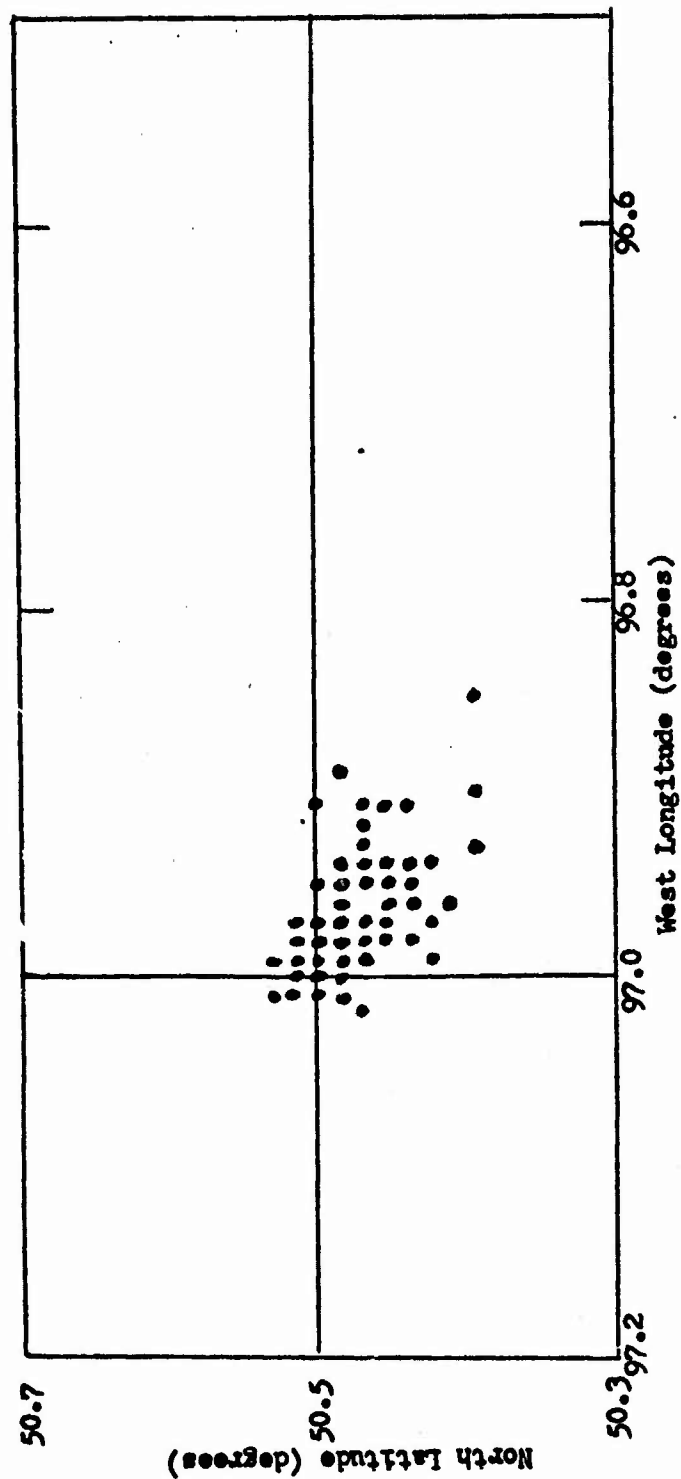
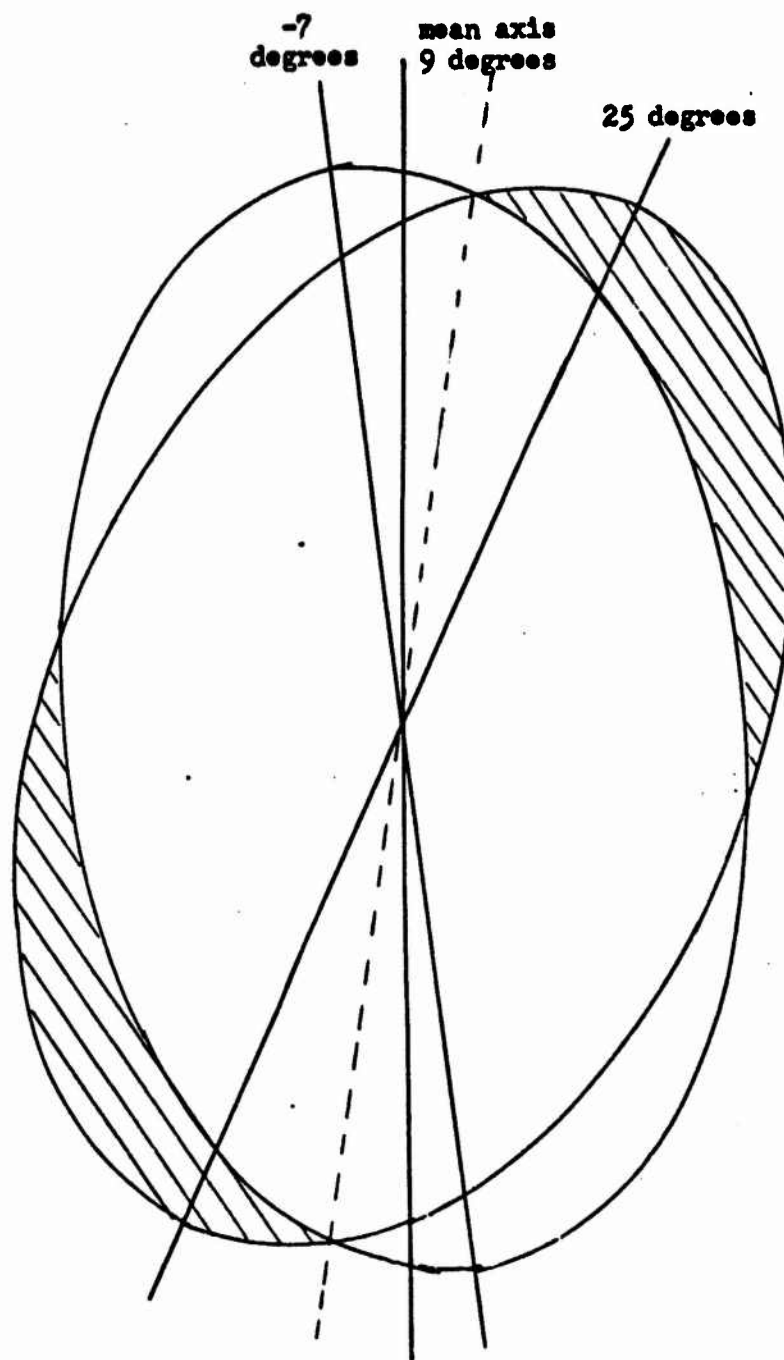


FIGURE 12



Shaded area is that displaced by a 32 degree rotation of axis of ellipse with semimajor axis = 2.92 and semi-minor axis = 1.90.

FIGURE 13

APPENDIX A

TABLE 1

Distance (miles)	b' Maxima (degrees)
0-50	0.0
50-900	3.0
900-1800	2.5
1800-2700	2.0
2700-3600	1.5
> 3600	0.0

Maxima assigned for the calculation of means for the component of bearing error due to ionospheric tilt as a function of distance.

TABLE II

Station	Location	
	Lat.	Lon.
Miami	25.6	80.2
Boston	42.4	71.0
Grand Falls	48.0	94.0
Seattle	47.5	122.5
Los Angeles	34.0	118.5
Houston	30.0	97.9

Composition of RDF network for simulation

TABLE III

Target	Location	
	Lat.	Lon.
Omaha	41.2	96.0
Veracruz	18.5	96.0
Gimli	50.5	97.0
Atlantic	35.0	58.0
Pacific	40.0	135.0

Targets used in simulation

TABLE IV

Location				90 Percent Confidence Ellipse					
Lat.	SD	Lon.	SD	Major Semiaxis	SD	Minor Semiaxis	SD	Axis of Rotation	SD
41.206	0.022	96.039	0.124	1.295	0.006	1.189	0.005	11.124	3.694
41.191	0.019	95.964	0.136	1.296	0.006	1.189	0.005	11.599	3.538
41.187	0.029	96.019	0.149	1.295	0.008	1.190	0.006	10.742	3.506
41.170	0.023	95.996	0.138	1.296	0.007	1.189	0.006	10.454	3.755
41.164	0.021	95.960	0.138	1.294	0.007	1.190	0.006	10.343	3.957
41.156	0.021	95.997	0.155	1.294	0.007	1.191	0.006	10.948	3.242
41.147	0.022	95.984	0.138	1.295	0.008	1.190	0.006	10.517	2.936
41.139	0.020	95.999	0.150	1.295	0.008	1.190	0.006	10.253	4.116
41.124	0.022	95.972	0.157	1.296	0.007	1.189	0.006	10.562	3.756
41.115	0.023	95.991	0.148	1.296	0.007	1.189	0.005	10.811	3.188
41.199	0.019	95.998	0.144	1.297	0.006	1.188	0.005	11.686	3.596
41.199	0.025	95.991	0.146	1.294	0.006	1.197	0.007	11.108	3.970
41.185	0.024	95.993	0.142	1.294	0.007	1.190	0.006	11.106	3.539
41.177	0.021	96.012	0.127	1.295	0.006	1.190	0.005	10.027	3.753
41.165	0.019	96.021	0.145	1.296	0.006	1.189	0.005	11.190	3.386
41.155	0.023	96.023	0.140	1.295	0.007	1.189	0.005	10.842	3.645
41.148	0.024	96.014	0.128	1.295	0.007	1.190	0.006	10.445	3.506
41.133	0.020	95.998	0.140	1.295	0.006	1.190	0.005	9.985	4.764
41.123	0.021	96.005	0.157	1.297	0.007	1.188	0.005	11.283	3.528
41.115	0.025	95.971	0.131	1.295	0.008	1.190	0.006	9.916	3.823
41.108	0.022	96.017	0.125	1.296	0.006	1.189	0.004	10.046	3.053
41.098	0.020	95.992	0.130	1.295	0.006	1.189	0.005	11.090	3.961
41.090	0.021	96.010	0.137	1.296	0.007	1.189	0.005	11.408	3.400
41.089	0.019	96.001	0.112	1.293	0.007	1.191	0.005	9.772	4.383
41.077	0.030	96.014	0.130	1.295	0.008	1.190	0.006	10.921	3.399

Sample means and standard deviations

Target: Omaha

Mode: No tilt

All values in degrees

TABLE V

Location				90 Percent Confidence Ellipse					
Lat.	SD	Lon.	SD	Major Semiaxis	SD	Minor Semiaxis	SD	Axis of Rotation	SD
41.195	0.018	96.031	0.151	1.294	0.006	1.191	0.005	8.126	3.743
41.192	0.014	95.973	0.166	1.294	0.006	1.190	0.005	7.483	3.683
41.181	0.015	96.009	0.117	1.293	0.007	1.191	0.006	7.818	3.582
41.166	0.015	96.014	0.014	1.296	0.006	1.189	0.005	9.518	4.011
41.156	0.016	95.974	0.119	1.295	0.007	1.190	0.005	8.567	4.143
41.153	0.017	95.978	0.145	1.294	0.006	1.191	0.005	7.644	3.484
41.138	0.013	95.980	0.141	1.297	0.006	1.188	0.005	8.300	3.593
41.139	0.021	95.974	0.147	1.294	0.006	1.191	0.005	7.454	4.493
41.126	0.016	95.957	0.116	1.295	0.005	1.190	0.004	9.060	4.178
41.120	0.022	95.980	0.147	1.294	0.006	1.190	0.005	8.832	4.195
41.106	0.019	95.986	0.164	1.294	0.006	1.191	0.004	8.493	5.166
41.097	0.019	95.996	0.127	1.295	0.007	1.190	0.005	8.874	4.049
41.091	0.017	95.960	0.122	1.294	0.006	1.190	0.004	8.641	3.905
41.082	0.017	95.938	0.141	1.294	0.006	1.190	0.005	8.977	3.561
41.071	0.016	95.956	0.160	1.294	0.006	1.191	0.005	8.913	3.594
41.190	0.016	95.948	0.139	1.295	0.006	1.190	0.005	8.802	3.578
41.177	0.020	96.016	0.135	1.295	0.006	1.190	0.005	7.813	3.698
41.173	0.022	95.983	0.160	1.293	0.006	1.191	0.005	7.959	3.757
41.161	0.019	95.993	0.176	1.295	0.007	1.190	0.005	8.329	3.804
41.153	0.015	95.969	0.146	1.294	0.006	1.191	0.005	7.836	4.222
41.142	0.013	95.968	0.114	1.295	0.005	1.190	0.004	9.612	3.686
41.138	0.017	95.970	0.120	1.294	0.006	1.191	0.004	8.833	3.758
41.127	0.015	96.005	0.130	1.295	0.006	1.190	0.005	9.050	3.817
41.108	0.019	95.965	0.125	1.293	0.005	1.191	0.004	8.143	3.953
41.112	0.015	95.971	0.160	1.296	0.006	1.189	0.005	8.538	3.522

Sample means and standard deviations

Target: Omaha

Mode: Tilt

All values in degrees

TABLE VI

Location				90 Percent Confidence Ellipse					
Lat.	SD	Lon.	SD	Major Semiaxis	SD	Minor Semiaxis	SD	Axis of Rotation	SD
35.082	0.251	57.803	0.551	3.826	0.089	0.900	0.001	-25.747	0.280
35.027	0.225	57.918	0.535	3.820	0.092	0.900	0.001	-25.848	0.283
34.980	0.232	58.056	0.483	3.867	0.069	0.899	0.001	-25.821	0.260
35.025	0.227	57.913	0.560	3.836	0.087	0.900	0.001	-25.831	0.302
34.988	0.241	58.018	0.534	3.853	0.089	0.900	0.001	-25.874	0.301
35.020	0.201	57.850	0.506	3.828	0.093	0.900	0.001	-25.757	0.311
34.956	0.192	58.025	0.521	3.853	0.101	0.900	0.001	-25.857	0.303
34.954	0.220	58.013	0.519	3.838	0.089	0.900	0.001	-25.892	0.324
34.976	0.221	57.924	0.495	3.831	0.071	0.900	0.001	-25.859	0.259
34.972	0.240	57.894	0.592	3.821	0.094	0.900	0.001	-25.847	0.299
34.936	0.206	58.012	0.510	3.843	0.095	0.900	0.001	-25.866	0.300
34.943	0.194	57.869	0.466	3.812	0.086	0.900	0.001	-25.783	0.358
34.982	0.251	57.892	0.563	3.832	0.090	0.900	0.001	-25.919	0.324
34.932	0.242	57.864	0.551	3.820	0.090	0.900	0.001	-25.789	0.269
34.927	0.258	57.895	0.633	3.811	0.098	0.900	0.001	-25.867	0.322
34.938	0.218	57.807	0.578	3.812	0.016	0.900	0.001	-25.759	0.269
34.877	0.228	57.904	0.605	3.819	0.101	0.900	0.001	-25.801	0.321
34.903	0.249	57.888	0.542	3.813	0.085	0.900	0.001	-25.877	0.267
34.910	0.204	57.878	0.495	3.815	0.089	0.900	0.001	-25.891	0.302
34.839	0.240	58.013	0.590	3.829	0.107	0.900	0.001	-25.930	0.291
35.045	0.248	57.846	0.578	3.840	0.107	0.900	0.001	-25.670	0.308
35.026	0.211	57.945	0.541	3.841	0.093	0.900	0.001	-25.809	0.307
35.041	0.238	57.912	0.595	3.848	0.092	0.900	0.001	-25.758	0.329
35.001	0.210	57.952	0.581	3.836	0.099	0.900	0.001	-25.843	0.283
34.988	0.213	57.968	0.528	3.837	0.092	0.900	0.001	-25.838	0.352

Sample means and standard deviations

Target: Atlantic

Mode: No tilt

All values in degrees

TABLE VII

Location				90 Percent Confidence Ellipse					
Lat.	SD	Lon.	SD	Major Semiaxis	SD	Minor Semiaxis	SD	Axis of Rotation	SD
34.995	0.167	58.028	0.365	3.777	0.085	0.901	0.001	-26.142	0.219
35.023	0.135	57.952	0.320	3.772	0.072	0.901	0.001	-26.030	0.211
35.022	0.157	57.946	0.341	3.782	0.071	0.901	0.001	-26.070	0.197
35.001	0.115	57.921	0.270	3.756	0.086	0.901	0.001	-26.103	0.209
35.017	0.153	57.878	0.313	3.740	0.090	0.901	0.001	-26.168	0.228
34.962	0.153	57.950	0.401	3.752	0.085	0.901	0.001	-26.149	0.232
34.931	0.157	58.077	0.385	3.777	0.068	0.901	0.001	-26.220	0.254
34.979	0.161	57.950	0.384	3.781	0.075	0.901	0.001	-26.137	0.220
34.971	0.166	57.947	0.372	3.749	0.096	0.901	0.001	-26.220	0.211
34.970	0.186	57.891	0.411	3.744	0.088	0.901	0.001	-26.178	0.243
34.939	0.154	57.940	0.358	3.758	0.078	0.901	0.001	-26.165	0.246
34.925	0.140	57.947	0.309	3.752	0.067	0.901	0.001	-26.175	0.199
34.895	0.136	58.044	0.328	3.751	0.074	0.901	0.001	-26.241	0.205
34.927	0.161	57.907	0.342	3.741	0.071	0.901	0.001	-26.200	0.207
34.900	0.126	57.956	0.366	3.751	0.079	0.901	0.001	-26.201	0.221
35.046	0.111	57.933	0.270	3.772	0.068	0.901	0.001	-26.107	0.184
35.013	0.172	57.947	0.440	3.757	0.093	0.901	0.001	-26.128	0.251
34.977	0.142	58.023	0.346	3.778	0.082	0.901	0.001	-26.139	0.180
35.019	0.182	57.921	0.354	3.767	0.084	0.901	0.001	-26.131	0.215
35.026	0.151	57.877	0.384	3.768	0.083	0.901	0.001	-26.088	0.223
34.960	0.168	58.009	0.392	3.770	0.088	0.901	0.001	-26.186	0.224
35.004	0.119	57.882	0.293	3.745	0.076	0.901	0.001	-26.183	0.168
34.982	0.158	57.927	0.349	3.757	0.081	0.901	0.001	-26.163	0.201
34.952	0.174	57.928	0.348	3.744	0.072	0.901	0.001	-26.192	0.223
34.935	0.140	57.973	0.364	3.752	0.083	0.901	0.001	-26.214	0.225

Sample means and standard deviations

Target: Atlantic

Mode: Tilt

All values in degrees

TABLE VIII

Location				90 Percent Confidence Ellipse					
Lat.	SD	Lon.	SD	Major Semiaxis	SD	Minor Semiaxis	SD	Axis of Rotation	SD
40.024	0.152	135.044	0.502	3.552	0.097	0.904	0.002	20.651	0.326
40.049	0.154	135.140	0.580	3.584	0.105	0.904	0.002	20.721	0.289
40.013	0.181	134.981	0.703	3.583	0.088	0.904	0.002	20.747	0.317
39.971	0.163	134.889	0.585	3.380	0.087	0.904	0.001	20.658	0.397
40.027	0.183	135.083	0.641	3.584	0.098	0.904	0.002	20.639	0.309
40.002	0.179	135.034	0.631	3.591	0.096	0.903	0.002	20.633	0.333
40.008	0.148	135.001	0.522	3.592	0.084	0.903	0.001	20.788	0.260
40.031	0.169	135.096	0.614	3.591	0.084	0.903	0.001	20.692	0.359
39.980	0.160	134.884	0.562	3.596	0.086	0.903	0.001	20.697	0.266
40.008	0.160	135.008	0.557	3.576	0.093	0.904	0.002	20.699	0.326
40.011	0.143	135.016	0.549	3.602	0.092	0.903	0.001	20.753	0.296
39.983	0.190	134.919	0.674	3.600	0.093	0.903	0.002	20.723	0.292
40.037	0.179	135.110	0.639	3.610	0.083	0.903	0.001	20.748	0.333
39.996	0.168	134.977	0.645	3.596	0.097	0.903	0.002	20.674	0.308
39.965	0.186	134.906	0.647	3.589	0.090	0.903	0.001	20.796	0.326
40.008	0.170	135.006	0.587	3.559	0.083	0.904	0.001	20.654	0.284
40.028	0.168	135.028	0.625	3.620	0.091	0.903	0.001	20.697	0.306
40.022	0.179	135.054	0.642	3.571	0.069	0.904	0.001	20.693	0.293
40.000	0.203	135.030	0.754	3.593	0.113	0.903	0.002	20.735	0.354
40.018	0.185	135.053	0.670	3.564	0.076	0.904	0.001	20.684	0.341
40.032	0.203	135.090	0.721	3.568	0.082	0.904	0.001	20.689	0.317
40.015	0.193	135.035	0.677	3.592	0.078	0.903	0.001	20.702	0.327
40.008	0.194	134.998	0.616	3.598	0.088	0.903	0.001	20.701	0.359
40.016	0.157	135.017	0.631	3.603	0.084	0.903	0.001	20.739	0.306
40.025	0.144	135.032	0.583	3.582	0.101	0.904	0.002	20.652	0.409

Sample means and standard deviations

Target: Pacific

Mode: No tilt

The dimension of all values is degrees

TABLE IX

Location				90 Percent Confidence Ellipse					
Lat.	SD	Lon.	SD	Major Semiaxis	SD	Minor Semiaxis	SD	Axis of Rotation	SD
40.000	0.102	134.963	0.417	3.425	0.060	0.906	0.001	20.712	0.272
39.984	0.081	134.945	0.350	3.446	0.064	0.906	0.001	20.698	0.268
39.982	0.074	134.901	0.281	3.456	0.054	0.906	0.001	20.740	0.266
39.987	0.080	134.895	0.342	3.444	0.072	0.906	0.001	20.686	0.201
39.997	0.081	134.987	0.346	3.447	0.073	0.906	0.001	20.607	0.264
39.997	0.074	134.998	0.337	3.441	0.067	0.906	0.001	20.623	0.233
39.968	0.075	134.867	0.298	3.435	0.080	0.906	0.001	20.669	0.278
39.997	0.087	134.977	0.375	3.450	0.069	0.906	0.001	20.705	0.258
40.001	0.094	134.971	0.327	3.440	0.067	0.906	0.001	20.647	0.296
39.985	0.104	134.912	0.402	3.452	0.077	0.906	0.001	20.699	0.301
40.033	0.084	135.077	0.357	3.453	0.070	0.906	0.001	20.669	0.289
40.003	0.095	135.010	0.404	3.437	0.076	0.906	0.001	20.608	0.313
40.002	0.077	134.985	0.302	3.437	0.069	0.906	0.001	20.649	0.271
39.997	0.077	134.980	0.332	3.452	0.082	0.906	0.001	20.617	0.262
40.020	0.100	135.043	0.409	3.462	0.069	0.906	0.001	20.636	0.248
40.010	0.079	135.090	0.338	3.420	0.073	0.906	0.001	20.598	0.324
39.996	0.102	135.009	0.383	3.438	0.072	0.906	0.001	20.558	0.270
39.991	0.090	134.951	0.336	3.439	0.057	0.906	0.001	20.674	0.336
39.996	0.084	134.934	0.296	3.452	0.080	0.906	0.001	20.666	0.295
39.978	0.091	134.906	0.388	3.430	0.072	0.906	0.001	20.676	0.274
39.997	0.081	134.958	0.351	3.453	0.064	0.906	0.001	20.702	0.291
40.005	0.103	135.006	0.396	3.433	0.080	0.906	0.001	20.580	0.268
39.999	0.090	134.954	0.353	3.451	0.074	0.906	0.001	20.621	0.257
40.008	0.078	135.010	0.318	3.450	0.067	0.906	0.001	20.653	0.282
39.984	0.093	134.908	0.347	3.463	0.077	0.906	0.001	20.676	0.315

Sample means and standard deviations

Target: Pacific

Mode: Tilt

All values in degrees

TABLE X

Location				90 Percent Confidence Ellipse					
Lat.	SD	Lon.	SD	Major Semiaxis	SD	Minor Semiaxis	SD	Axis of Rotation	SD
50.483	0.024	96.970	0.063	1.415	0.008	1.116	0.004	33.967	1.153
50.473	0.030	96.975	0.072	1.415	0.010	1.116	0.005	34.088	1.068
50.460	0.032	96.977	0.051	1.418	0.010	1.114	0.005	33.580	1.240
50.452	0.030	96.979	0.053	1.418	0.009	1.114	0.004	33.743	1.353
50.439	0.045	96.962	0.112	1.417	0.009	1.115	0.005	33.680	1.206
50.437	0.033	96.977	0.071	1.417	0.008	1.115	0.004	33.703	1.262
50.424	0.039	96.970	0.086	1.418	0.012	1.114	0.006	33.489	1.218
50.407	0.038	96.953	0.112	1.419	0.010	1.114	0.005	33.275	1.059
50.401	0.033	96.977	0.053	1.419	0.012	1.114	0.006	33.157	1.005
50.395	0.035	96.968	0.079	1.418	0.010	1.114	0.005	33.297	1.050
50.389	0.034	96.975	0.067	1.420	0.010	1.113	0.005	33.001	0.904
50.378	0.031	96.981	0.057	1.420	0.010	1.113	0.005	33.439	1.312
50.376	0.025	96.988	0.026	1.421	0.007	1.113	0.004	32.728	0.938
50.362	0.034	96.967	0.034	1.422	0.011	1.112	0.005	32.943	1.148
50.359	0.038	96.962	0.124	1.421	0.011	1.113	0.005	33.149	1.385
50.479	0.036	96.954	0.098	1.416	0.008	1.115	0.004	33.913	1.191
50.468	0.037	96.962	0.105	1.416	0.008	1.115	0.004	33.842	1.397
50.455	0.045	96.962	0.114	1.419	0.011	1.114	0.005	33.076	1.331
50.455	0.031	96.975	0.061	1.418	0.009	1.114	0.004	33.631	1.068
50.437	0.038	96.957	0.091	1.419	0.011	1.114	0.005	33.528	1.213
50.424	0.037	96.949	0.113	1.419	0.010	1.114	0.005	33.860	1.158
50.428	0.030	96.980	0.060	1.419	0.009	1.114	0.004	33.467	1.151
50.419	0.024	96.986	0.034	1.418	0.008	1.114	0.004	33.447	1.343
50.402	0.033	96.966	0.082	1.420	0.010	1.113	0.005	33.309	1.092
50.404	0.027	96.985	0.031	1.416	0.009	1.115	0.004	33.203	1.237

Sample means and standard deviations

Target: Gimli

Mode: No tilt

All values in degrees

TABLE XI

Location				90 Percent Confidence Ellipse					
Lat.	SD	Lon.	SD	Major Semiaxis	SD	Minor Semiaxis	SD	Axis of Rotation	SD
50.468	0.034	96.959	0.041	1.420	0.010	1.113	0.005	30.952	1.273
50.462	0.026	96.970	0.027	1.418	0.011	1.114	0.005	31.338	1.182
50.455	0.028	96.974	0.033	1.420	0.007	1.113	0.003	31.278	1.099
50.439	0.030	96.963	0.032	1.420	0.009	1.113	0.004	31.443	1.076
50.436	0.027	96.970	0.032	1.418	0.007	1.114	0.004	31.448	1.239
50.427	0.028	96.962	0.064	1.419	0.005	1.114	0.005	31.185	1.060
50.409	0.030	96.962	0.029	1.420	0.009	1.113	0.004	30.843	1.022
50.410	0.029	96.971	0.031	1.419	0.010	1.114	0.005	30.736	1.204
50.396	0.025	96.972	0.026	1.420	0.008	1.113	0.004	30.712	1.002
50.388	0.028	96.969	0.025	1.420	0.010	1.114	0.005	30.696	1.154
50.387	0.028	96.967	0.031	1.419	0.012	1.114	0.006	30.510	1.168
50.369	0.035	96.965	0.031	1.421	0.012	1.113	0.005	30.536	1.315
50.365	0.022	96.969	0.026	1.419	0.009	1.114	0.004	30.440	1.038
50.355	0.021	96.974	0.026	1.419	0.009	1.114	0.005	30.629	0.794
50.346	0.032	96.972	0.036	1.420	0.010	1.113	0.005	30.179	1.065
50.463	0.032	96.975	0.031	1.418	0.010	1.114	0.005	31.873	1.088
50.448	0.031	96.960	0.033	1.420	0.010	1.113	0.005	31.076	1.044
50.445	0.026	96.967	0.027	1.418	0.010	1.114	0.005	31.198	1.133
50.430	0.035	96.970	0.036	1.419	0.010	1.114	0.005	31.175	1.151
50.428	0.024	96.968	0.034	1.418	0.010	1.114	0.005	30.908	1.091
50.415	0.027	96.972	0.024	1.419	0.009	1.114	0.004	31.053	1.140
50.409	0.026	96.975	0.030	1.419	0.008	1.114	0.004	30.950	0.910
50.409	0.023	96.975	0.023	1.418	0.008	1.114	0.004	30.913	1.137
50.385	0.033	96.964	0.032	1.420	0.012	1.113	0.006	30.767	1.078
50.377	0.030	96.967	0.029	1.422	0.011	1.112	0.005	30.484	1.065

Sample means and standard deviations

Target: Gimli

Mode: Tilt

All values in degrees

TABLE XII

Location				90 Percent Confidence Ellipse					
Lat.	SD	Lon.	SD	Major Semi-axis	SD	Minor Semi-axis	SD	Axis of Rotation	SD
18.501	0.051	95.998	0.093	1.538	0.011	1.066	0.004	-86.310	0.743
18.489	0.040	95.995	0.036	1.540	0.012	1.065	0.004	-86.469	0.714
18.499	0.059	95.977	0.105	1.542	0.013	1.065	0.004	-86.37	0.684
18.476	0.045	95.005	0.041	1.542	0.012	1.065	0.004	-86.600	0.557
18.491	0.055	95.968	0.129	1.540	0.013	1.065	0.004	-86.349	0.870
18.457	0.053	96.007	0.047	1.541	0.011	1.065	0.004	-86.454	0.657
18.463	0.051	95.984	0.100	1.542	0.012	1.065	0.004	-86.471	0.682
18.454	0.042	95.996	0.041	1.542	0.012	1.065	0.004	-86.437	0.630
18.450	0.065	95.966	0.142	1.544	0.011	1.065	0.004	-86.553	0.641
18.424	0.044	95.995	0.059	1.541	0.011	1.065	0.004	-86.509	0.654
18.422	0.049	95.988	0.042	1.545	0.010	1.064	0.003	-86.463	0.647
18.409	0.055	95.979	0.150	1.538	0.013	1.066	0.004	-86.558	0.632
18.406	0.043	95.995	0.051	1.543	0.010	1.064	0.003	-86.505	0.696
18.398	0.053	95.984	0.107	1.542	0.011	1.065	0.004	-86.424	0.667
18.387	0.059	95.970	0.106	1.542	0.013	1.065	0.004	-86.444	0.676
18.504	0.049	95.992	0.035	1.541	0.010	1.065	0.003	-86.369	0.663
18.501	0.047	95.998	0.045	1.542	0.014	1.065	0.005	-86.378	0.715
18.499	0.065	95.962	0.149	1.539	0.011	1.066	0.004	-86.288	0.743
18.492	0.054	95.980	0.054	1.540	0.012	1.065	0.004	-86.385	0.676
18.479	0.061	95.975	0.111	1.542	0.012	1.065	0.004	-86.337	0.753
18.466	0.065	95.968	0.175	1.538	0.012	1.066	0.004	-86.413	0.722
18.453	0.044	06.002	0.037	1.541	0.010	1.065	0.003	-86.449	0.600
18.451	0.058	95.991	0.089	1.541	0.012	1.065	0.004	-86.516	0.619
18.431	0.045	95.998	0.037	1.543	0.010	1.064	0.003	-86.480	0.721
18.429	0.053	95.996	0.071	1.542	0.012	1.065	0.004	-86.669	0.662

Sample means and standard deviations

Target: Veracruz

Mode: No tilt

All values in degrees

**TABLE XIII**

Location				90 Percent Confidence Ellipse					
Lat.	SD	Lon.	SD	Major Semiaxis	SD	Minor Semiaxis	SD	Axis of Rotation	SD
18.588	0.067	95.868	0.220	1.565	0.011	1.057	0.003	-86.989	0.707
18.574	0.075	95.872	0.245	1.562	0.009	1.058	0.003	-87.139	0.595
18.568	0.087	95.858	0.256	1.562	0.009	1.058	0.003	-86.917	0.668
18.522	0.057	95.934	0.150	1.563	0.010	1.058	0.003	-87.028	0.569
18.516	0.063	95.952	0.126	1.562	0.009	1.058	0.003	-87.097	0.493
18.530	0.067	95.882	0.254	1.561	0.009	1.058	0.003	-87.129	0.724
18.506	0.046	95.963	0.073	1.566	0.010	1.057	0.003	-87.240	0.688
18.525	0.081	95.844	0.270	1.564	0.011	1.058	0.003	-87.087	0.601
18.497	0.058	95.909	0.195	1.567	0.009	1.057	0.003	-87.180	0.605
18.489	0.080	95.881	0.272	1.565	0.012	1.057	0.004	-87.211	0.709
18.483	0.067	95.904	0.175	1.564	0.010	1.058	0.003	-87.073	0.765
18.469	0.086	95.874	0.271	1.565	0.010	1.057	0.003	-87.189	0.648
18.460	0.077	95.887	0.239	1.566	0.008	1.057	0.003	-87.361	0.567
18.438	0.061	95.918	0.284	1.565	0.009	1.057	0.003	-87.299	0.548
18.441	0.062	95.927	0.169	1.567	0.011	1.057	0.003	-87.177	0.694
18.571	0.067	95.910	0.191	1.560	0.010	1.059	0.003	-86.989	0.529
18.544	0.043	95.970	0.062	1.560	0.011	1.059	0.003	-87.019	0.708
18.566	0.085	95.845	0.292	1.564	0.009	1.058	0.003	-87.135	0.739
18.539	0.075	95.935	0.152	1.563	0.010	1.058	0.003	-87.069	0.612
18.521	0.069	95.945	0.205	1.564	0.011	1.058	0.003	-87.157	0.656
18.531	0.069	95.899	0.222	1.564	0.011	1.058	0.003	-87.196	0.649
18.504	0.059	95.926	0.154	1.565	0.012	1.057	0.004	-87.072	0.523
18.502	0.057	95.918	0.197	1.564	0.010	1.058	0.003	-87.094	0.683
18.499	0.067	95.905	0.204	1.562	0.010	1.058	0.003	-87.084	0.643
18.472	0.056	95.968	0.095	1.565	0.010	1.057	0.003	-87.240	0.705

Sample means and standard deviations

Target: Veracruz

Mode: Tilt

All values in degrees

TABLE XIV

No tilt D(1)	Tilt D(1)
54.883	54.836
54.773	54.781
54.932	54.828
54.826	54.838
54.796	54.818
54.841	54.825
54.837	54.842
54.860	54.836
54.848	54.831
54.876	54.860
54.799	54.880
54.792	54.899
54.808	54.869
54.835	54.956
54.856	54.885
54.848	54.758
54.866	54.839
54.865	54.810
54.882	54.832
54.856	54.816
54.901	54.826
54.894	54.832
54.920	54.838
54.912	54.859
54.937	54.897

Reduced location data  
for the Omaha samples

## LIST OF REFERENCES

1. Ames, J.W., "Spacial Properties of Amplitude Fading of Continuous 17-Mc Radio Waves," Technical Report No. 87, Radioscience Laboratory, Stanford Electronics Laboratories, Stanford University, Stanford, California, March 1964.
2. Bain, W.C., "On the Rapidity of Fluctuation in Continuous-Wave Radio Bearings at High Frequencies," Institution of Electrical Engineers, B, 102, August 1955, pp. 541-543.
3. Barnum, J.R., "Mixed-Mode Oblique Ionograms: A Computer Ray-Tracing Interpretation," Technical Report No. 148, Radioscience Laboratory, Stanford Electronics Laboratories, Stanford University, Stanford, California, December 1968.
4. Bramley, E.N., and W. Ross, "Measurements of the Direction of Arrival of Short Radio Waves Reflected at the Ionosphere," Proceedings of the Royal Society of London, A, 207, June 1951, pp. 251-267.
5. Bramley, E.N., "Direction-Finding Studies of Large-Scale Ionospheric Irregularities," Proceedings of the Royal Society of London, A, 220, October 1953, pp. 39-61.
6. Bramley, E.N., "Some Aspects of the Rapid Directional Fluctuations of Short Radio Waves Reflected at the Ionosphere," Institution of Electrical Engineers, B, 102, August 1955, pp. 533-540.
7. Bramley, E.N., "Some Comparative Directional Measurements on Short Radio Waves over Different Transmission Paths," Institution of Electrical Engineers, B, 102, August 1955, pp. 544-549.
8. Bramley, E.N., "Directional Observations on H.F. Transmissions over 2100 Km.," Institution of Electrical Engineers, B, 103, May 1956, pp. 295-300.
9. Bredek, R.S., "A Method of Radiolocation Employing Around-the-World High Frequency Propagation," Illinois University, Engineering Experimental Station, Urbana, Illinois, Radiolocation Research Laboratory Report No. R.R.L.-214, August 1963.

10. Burt, W.A., D.J. Kaplan, R.R. Keenly, J.F. Reeves and F.B. Shaffer, "Mathematical Considerations Pertaining to the Accuracy of Position Location and Navigation Systems," NWRC, Stanford Research Institute, Menlo Park, California, April 1966.
11. Chan, K.L., and O.G. Villard, Jr., "Observations of Large-Scale Traveling Ionospheric Disturbances by Spaced-Path High-Frequency Instantaneous Frequency Measurements," Journal of Geophysical Research, 67, 3, March 1963, pp. 973-988.
12. Daniels, H.E., "The Theory of Position Finding," Journal of the Royal Statistical Society, B, 13, 2, 1951, pp. 186-207.
13. Davies, Kenneth, Ionospheric Radio Propagation, National Bureau of Standards Monograph 80, U.S. Government Printing Office, Washington, D.C., 1965.
14. Detert, D.G., "An Investigation of Large-Scale Ionospheric Disturbances in a Radiolocation Experiment," Illinois University, Engineering Experimental Station, Urbana, Illinois, Radiolocation Research Laboratory Publication No. 288, September 1965.
15. Haydon, G.W., and D.L. Lucas. "Predicting Ionospheric Electron Density Profiles," Radio Science, 3, 1, January 1968, pp. 111-119.
16. Heisler, L.H., "Observations of Movement of Perturbations in the F-Region," Journal of Atmospheric and Terrestrial Physics, 25, February 1963, pp. 71-86.
17. Heisler, L.H., "Experimental Studies of Perturbations in Ionospheric Plasma," Journal of Research of the National Bureau of Standards, 69D, 2, February 1965, pp. 219-225.
18. Hewish, A., "The Diffraction of Radio Waves in Passing Through a Phase-Changing Ionosphere," Proceedings of the Royal Society of London, A, 209, October 1951, pp. 81-96.
19. Hewish, A., "The Diffraction of Galactic Radio Waves as a Method of Investigating the Irregular Structure of the Ionosphere," Proceedings of the Royal Society of London, A, 214, October 1952, pp. 494-514.
20. Jones, R.M. "A Three-Dimensional Ray-Tracing Computer Program," Environmental Science Services Administration, Technical Report, Institute of Environmental Research-17/Institute of Telecommunications Sciences and Aeronomy -17, Institute of Telecommunications Sciences and Aeronomy, Boulder, Colorado, 1966.

21. Kelso, J.M., Radio Ray Propagation in the Ionosphere, McGraw-Hill, New York, 1964.
22. Kukes, I.S., and M. Ya. Starik, Principles of Radio Direction Finding, Soviet Radio Publishing House, Moscow, 1964.
23. Munro, G.H., and L. H. Heisler, "Ionosphere Dynamics," Proceedings of the Institute of Electrical and Electronics Engineers, Inc., 51, 11, November 1963, pp. 1475-1481.
24. Naylor, T.H., J.L. Balintfy, D.S. Burdick and K. Chu, Computer Simulation Techniques, John Wiley and Sons, New York, 1966.
25. Pope, J.W.R., "Measurement Processing in Position Locations Systems," Naval Security Group Activity, Skaggs Island, Sonoma, California, May 1970.
26. Pope, J.W.R., "A Vector Fix Procedure for High Frequency Direction Finding," Naval Security Group Activity, Skaggs Island, Sonoma, California, February 1971.
27. Stansfield, R.G., "Statistical Theory of D.F. Fixing," Journal of the Institution of Electrical Engineers, 94 3A, 15, 1947, pp. 762-770.
28. Sweeney, L.E., Jr., "Spacial Properties of Ionospheric Radio Propagation as Determined with Half-Degree Azimuthal Resolution," Technical Report No. 155, Radioscience Laboratory, Stanford Electronics Laboratories, Stanford University, Stanford, California, June 1970.
29. Thomas, P.D., "Spheroidal Geodesics, Reference Systems, and Local Geometry," SP-138, U.S. Naval Oceanographic Office, Washington, D.C., January 1970.